Tropical Built Environment Journal. Volume 14, No. 3, 48-64, 2026 www.tbejournal.com
ISSN: 1118-1790

Flood Detection, Extent Mapping and Susceptibility Assessment in Lokoja, Kogi State, Nigeria, Using Sentinel-1A SAR

Elijah S. Ebinne[1], Odike G. Onuche[1], and Ugwuoti Amos[1]

[1]Department of Geoinformatics and Surveying, University of Nigeria, Enugu Campus, Enugu State, Nigeria.

Corresponding author: odikegabriel@gmail.com

Abstract

Persistent cloud cover during the rainy season severely limits the usefulness of optical satellites for flood monitoring in tropical riverine environments. This study applied multi-temporal Sentinel-1 Synthetic Aperture Radar (SAR) data to detect and map flood extents, assess land-cover impacts, and generate a flood susceptibility map for the Niger-Benue confluence zone of Lokoja, Kogi State, Nigeria, during the 2018 and 2022 flood events. Ground Range Detected (GRD) images in dual polarisation (VV and VH) were pre-processed in SNAP and analysed using Otsu thresholding combined with multi-temporal change detection. Final flood extents were obtained by combining validated VV and VH masks after agreement analysis, slope masking (>8°), and connected-component filtering. Ancillary terrain and land-cover datasets were integrated for flood susceptibility mapping using Analytic Hierarchy Process (AHP) weighted multi-criteria evaluation. Results showed that the integrated flood extent increased from 198.45 km² in 2018 to 276.32 km² in 2022, representing a 39.2% rise. VH polarisation consistently mapped larger open-water areas than VV. Cropland accounted for 68.5% (2018) and 70.2% (2022) of the inundated area. Approximately 24% of the study area (≈747 km² of 3,181 km²) was classified as high or very high susceptibility. Accuracy assessment of the 2022 flood extent map (distinct from susceptibility mapping) yielded an overall accuracy of 84.0% and a Kappa coefficient of 0.68. The findings demonstrate that Sentinel-1 SAR provides reliable, weather-independent flood information suitable for operational monitoring in Lokoja and similar tropical confluence environments.

Keywords: Sentinel-1; SAR; flood extent mapping; dual polarisation; Lokoja; flood susceptibility; agricultural impact; Otsu thresholding

1. Introduction

Flooding is the most frequent and destructive natural hazard in Nigeria, with particularly severe impacts in Kogi State due to its location at the confluence of the Niger and Benue Rivers (NEMA, 2022, 2023). Optical remote sensing systems are frequently rendered ineffective during peak flood periods by persistent cloud cover. Synthetic Aperture Radar (SAR), especially the Sentinel-1 constellation, overcomes this limitation by operating

independently of weather and illumination conditions (Pulvirenti et al., 2024; Shen et al., 2019).

Several previous studies have applied Sentinel-1 SAR to flood mapping along the Niger–Benue system. Ebinne et al. (2019) and Agada et al. (2019) mapped the 2018 flood in Lokoja using threshold-based change detection and reported substantial inundation of buildings, roads and farmlands, but provided limited quantitative validation and did not produce susceptibility maps. Isiaka et al. (2023) assessed the 2022 flood in nearby Koton Karfe and quantified land-cover losses, yet the study did not include dual-polarisation comparison or multi-criteria susceptibility modelling. Broader reviews (Pulvirenti et al., 2024; Lang et al., 2024) highlight the value of semi-automatic thresholding and change detection but note that applications tailored to Nigerian confluence environments remain scarce. Consequently, a clear research gap exists for an integrated assessment that combines multi-year flood extent comparison, dual-polarisation analysis, quantitative land-cover impact assessment, and AHP-based susceptibility mapping within a single, validated framework for Lokoja.

1.1 Statement of the Research Problem

Lokoja continues to experience severe seasonal flooding, yet reliable, near-real-time spatial information for early warning and intervention planning remains insufficient. Optical satellite imagery is routinely unavailable during the cloudy peak-flood months, delaying assessments. Existing SAR studies in the area lack temporal comparison across major events, dual-polarisation analysis, formal susceptibility modelling, and rigorous accuracy assessment against independent reference data. These limitations constrain emergency response, land-use planning and long-term mitigation. There is therefore a pressing need for a SAR-based approach that delivers accurate flood extent maps and susceptibility information under the cloudy conditions typical of the Nigerian rainy season.

1.2 Aim and Objectives

The aim of this study is to detect and map flood extents, assess land-cover impacts, and generate a flood susceptibility map for Lokoja, Kogi State, using Sentinel-1A SAR data for the 2018 and 2022 flood events.

The specific objectives are to:

i. Acquire and pre-process multi-temporal Sentinel-1A GRD data for the 2018 and 2022 flood windows;

ii. Detect and delineate inundated areas using Otsu thresholding and multi-temporal change detection for both VV and VH polarisations;

iii. Combine the validated VV and VH flood masks and quantify the change in flood extent between 2018 and 2022;

iv. Assess the impact of flooding on land-cover classes using ESA WorldCover 2021;

v. Generate a flood susceptibility map using AHP-weighted multi-criteria evaluation of terrain and land-cover factors; and

vi. Validate the 2022 flood extent map against independent reference data and report accuracy metrics.

2. Study Area

Lokoja Local Government Area lies at the confluence of the Niger and Benue Rivers in north-central Nigeria (approximately 7°40′–8°00′ N, 6°30′–7°00′ E) and covers about 3,180 km². The climate is tropical wet-and-dry (Köppen Aw), with mean annual rainfall of 1,200–1,600 mm peaking between July and October. Low-lying alluvial floodplains dominate the landscape and support intensive agriculture. Flood risk is elevated by upstream dam releases (notably Lagdo Dam, Cameroon) that coincide with local peak rainfall (NEMA, 2022).

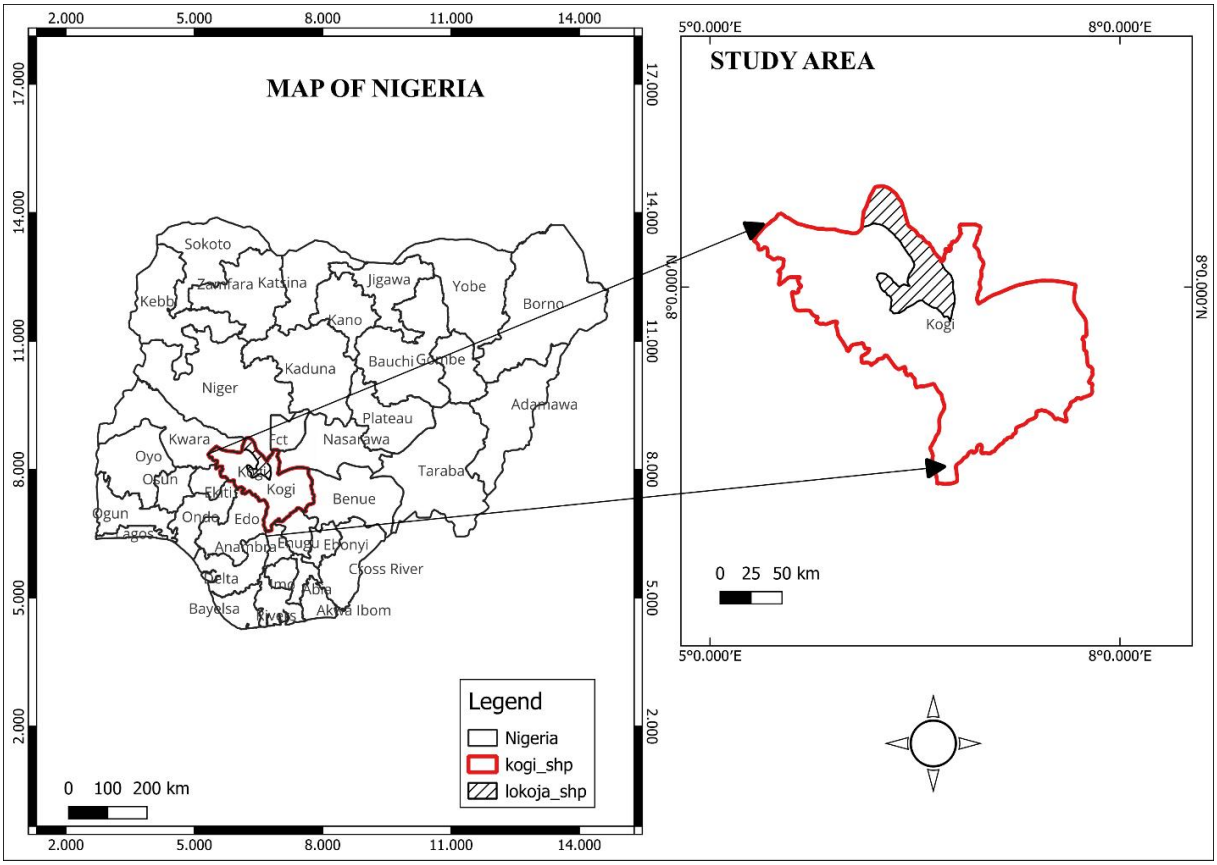


Figure 1: Location map of Lokoja LGA within Kogi State, Nigeria

3. Materials and Methods

3.1 Data

Sentinel-1A Ground Range Detected (GRD) images (ascending orbit, Interferometric Wide swath, dual VV+VH polarisation) covering the pre-flood (1 June–31 August) and peak-flood (15 September–15 November for 2018; 20 September–10 November for 2022) windows were acquired from the Copernicus Open Access Hub. Twenty pre-flood and 16 peak-flood images were used for 2018; 23 pre-flood and 10 peak-flood images were used for 2022. Median composites were generated for each window to suppress transient effects. Ancillary data comprised the SRTM 30 m Digital Elevation Model (DEM), ESA WorldCover 2021 land-cover product, and administrative boundaries. It is acknowledged that the single-date WorldCover 2021 layer was used for both years and therefore does not capture inter-annual land-cover change.

3.2 Pre-processing

All images were processed in the Sentinel Application Platform (SNAP) following the standard workflow: (i) precise orbit correction using restituted orbit files; (ii) radiometric calibration to sigma-nought (σ^0) in decibels; (iii) Lee-Sigma speckle filtering (5 × 5 window); and (iv) radiometric terrain correction using the SRTM DEM. The resulting backscatter images were subset to the study area boundary.

3.3 Flood Extraction and Combination of Polarizations

Flood extent was extracted independently for VV and VH using Otsu thresholding applied to the difference between pre-flood and peak-flood median composites. The automatically derived Otsu thresholds were –20.24 dB (VH) and –13.74 dB (VV) for 2018, and –19.24 dB (VH) and –14.25 dB (VV) for 2022. A slope mask (pixels with slope > 8°) was applied to remove high-terrain false positives, and connected-component filtering removed clusters smaller than 30 pixels. The two polarisation masks were then combined through agreement analysis: pixels classified as flooded by both channels, plus unique VH open-water detections after visual and reference-data verification, formed the final integrated flood extent. The validated extents adopted for subsequent analysis were 198.45 km² (2018) and 276.32 km² (2022).

3.4 Land-cover Impact Assessment

The integrated flood masks were intersected with the ESA WorldCover 2021 dataset to quantify the area and percentage of each land-cover class that was inundated. Note that the percentages reported represent the proportion of the mapped flooded area occupied by each class, not the proportion of the total class area that was flooded.

3.5 Flood Susceptibility Mapping

Flood susceptibility was mapped independently of the event-specific flood extents using Analytic Hierarchy Process (AHP) weighted linear combination of five factors: slope, elevation, Topographic Wetness Index (TWI), drainage density, and land use/land cover. Pairwise comparison yielded the following relative weights (consistency ratio < 0.10): elevation (0.32), slope (0.25), TWI (0.20), drainage density (0.13), and LULC (0.10). Factor layers were standardised to a common 0–1 scale and combined. The resulting susceptibility

index was classified into five zones (Very Low, Low, Moderate, High, Very High) using the Natural Breaks (Jenks) method. The susceptibility map covers the entire Lokoja LGA (3,181 km²) and is distinct from the event-specific flood extent maps; it was not subjected to the same pixel-based accuracy assessment.

3.6 Accuracy Assessment

A stratified random sample of 300 points (150 flooded, 150 non-flooded) was evaluated against independent reference data comprising NEMA flood situation reports, high-resolution optical imagery where cloud-free, and available field photographs. Overall accuracy, producer's and user's accuracies, and Cohen's Kappa coefficient were computed from the resulting confusion matrix. Only the 2022 flood extent map was validated in this manner; the susceptibility map was assessed qualitatively by visual comparison with the observed flood extents.

4. Results

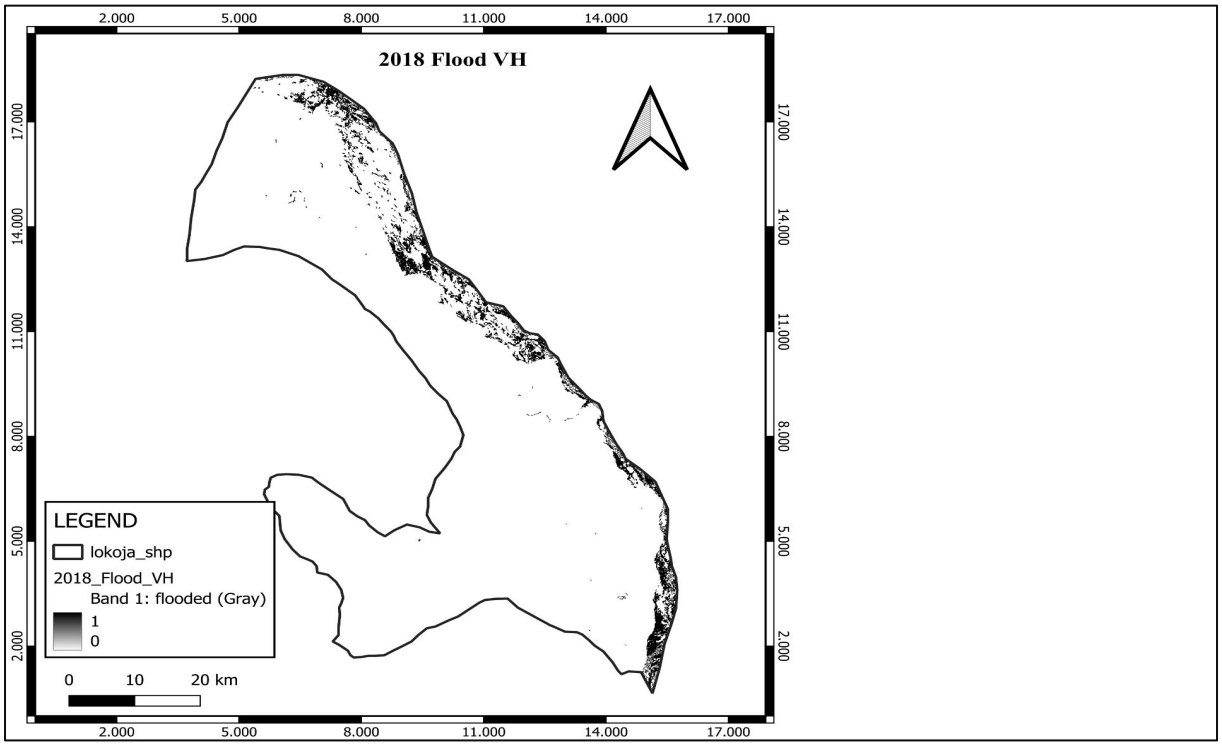
4.1 Flood Extent

Table 1 presents the polarisation-specific and integrated flood extents. VH consistently mapped larger areas than VV. After combination, slope masking and filtering, the final validated extents were 198.45 km² in 2018 and 276.32 km² in 2022, corresponding to a 39.2% increase. The expansion was most pronounced toward Koton-Karfe and Ibaji.

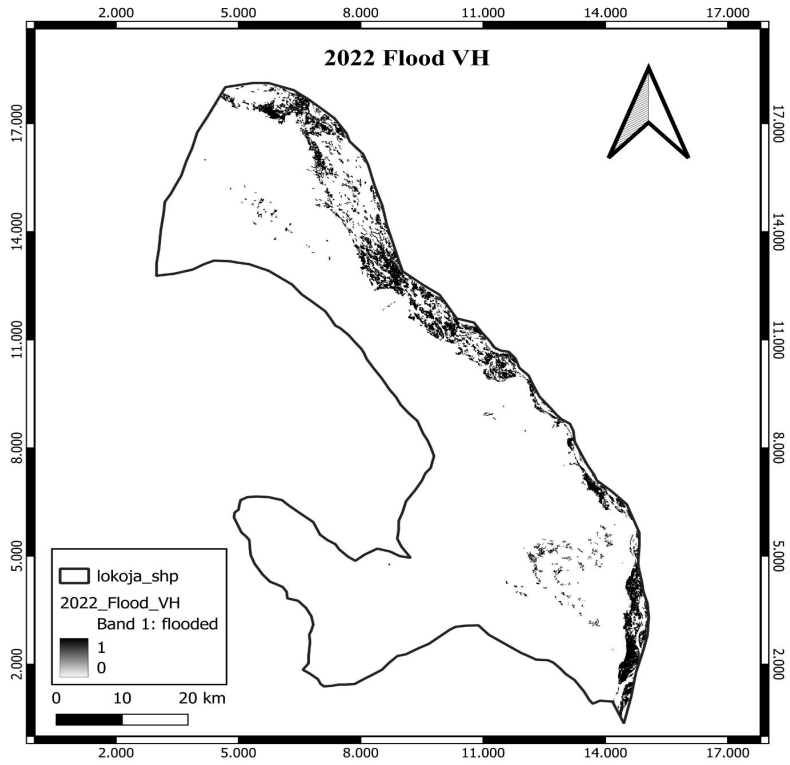
Table 1: Flood extent by polarisation and year

Year	VH extent (km²)	VV extent (km²)	VH − VV difference (km²)	Integrated validated extent (km²)
2018	208.52	190.69	17.83	198.45
2022	249.61	226.22	23.39	276.32

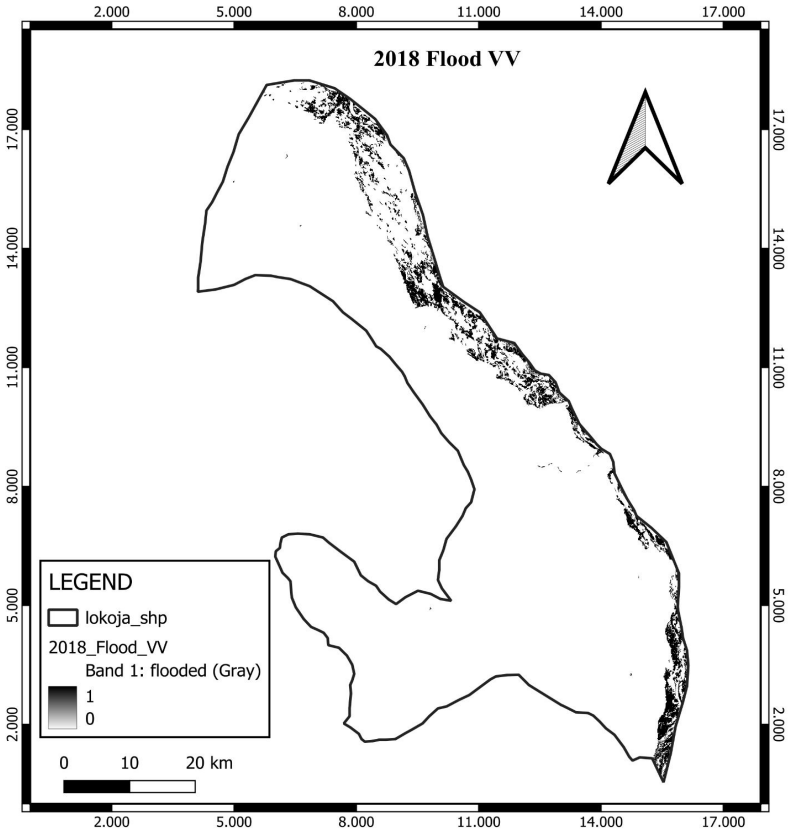
Agreement analysis showed that both channels classified the same pixels as flooded over 165.55 km² (2018) and 176.73 km² (2022). VH uniquely contributed the larger unique fraction in both years, supporting its use as the primary open-water indicator, with VV providing complementary information in vegetated and built-up margins.



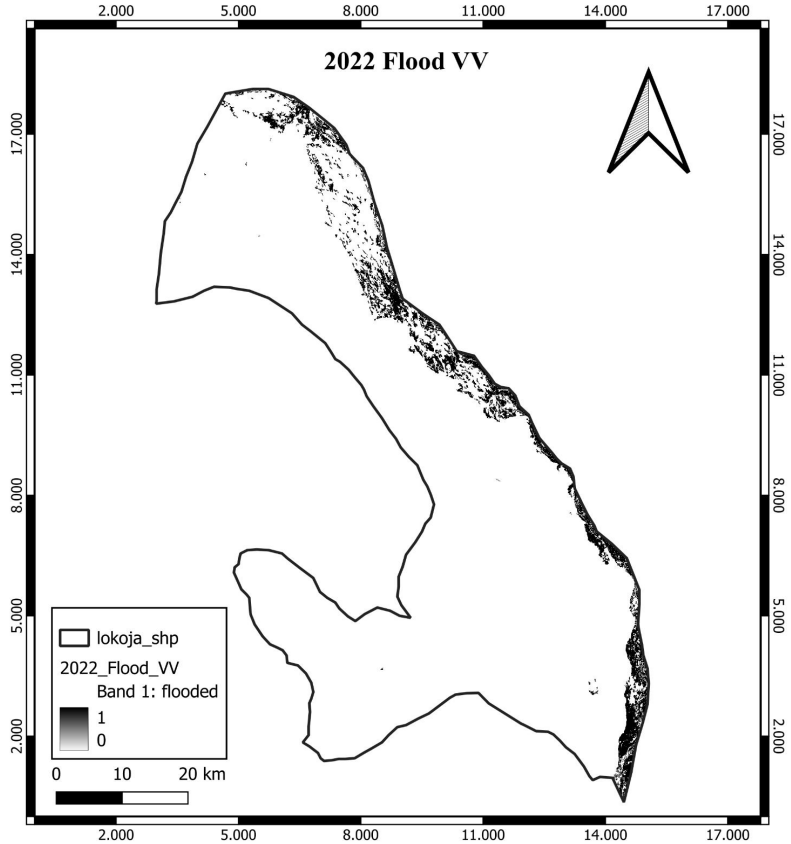
Figures 2: VH flood extent map for 2018



Figures 3: VH flood extent map for 2022



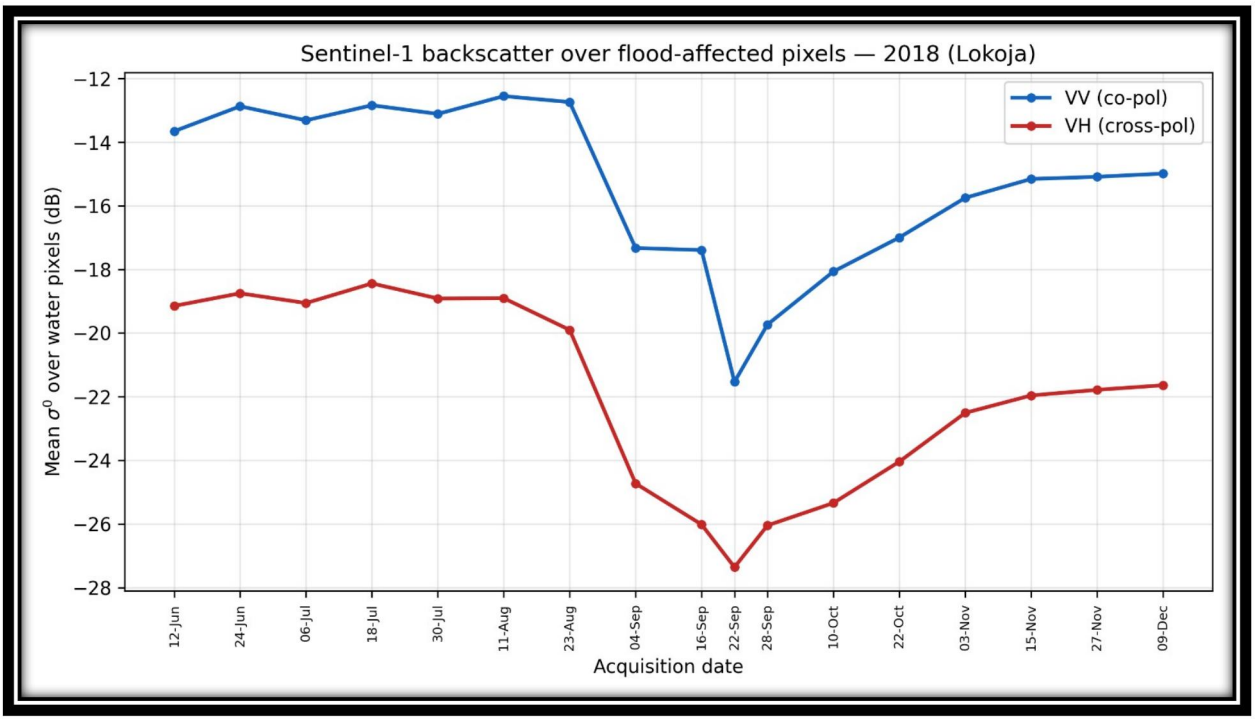
Figures 4: VV flood extent map for 2018



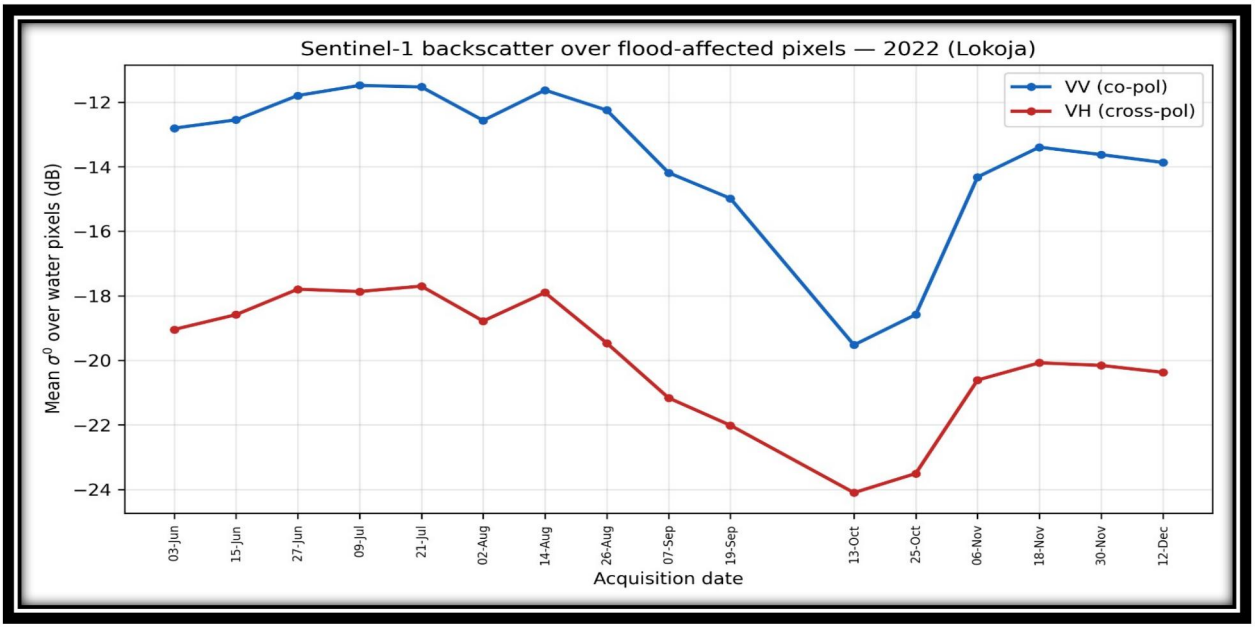
Figures 5: VV flood extent map for 2022

4.2 Backscatter Time Series

Mean backscatter declined sharply during peak flooding. In 2018 the lowest values occurred around 22 September (VH ≈ –27.4 dB; VV ≈ –21.5 dB). In 2022 the minimum was observed in mid-October (VH ≈ –24.1 dB; VV ≈ –19.5 dB). These reductions are consistent with specular reflection from smooth open water surfaces (Martinis & Rieke, 2015; Tsyganskaya et al., 2018; Pulvirenti et al., 2024).



Figures 6: Backscatter time-series -2018



Figures 7: Backscatter time-series -2022

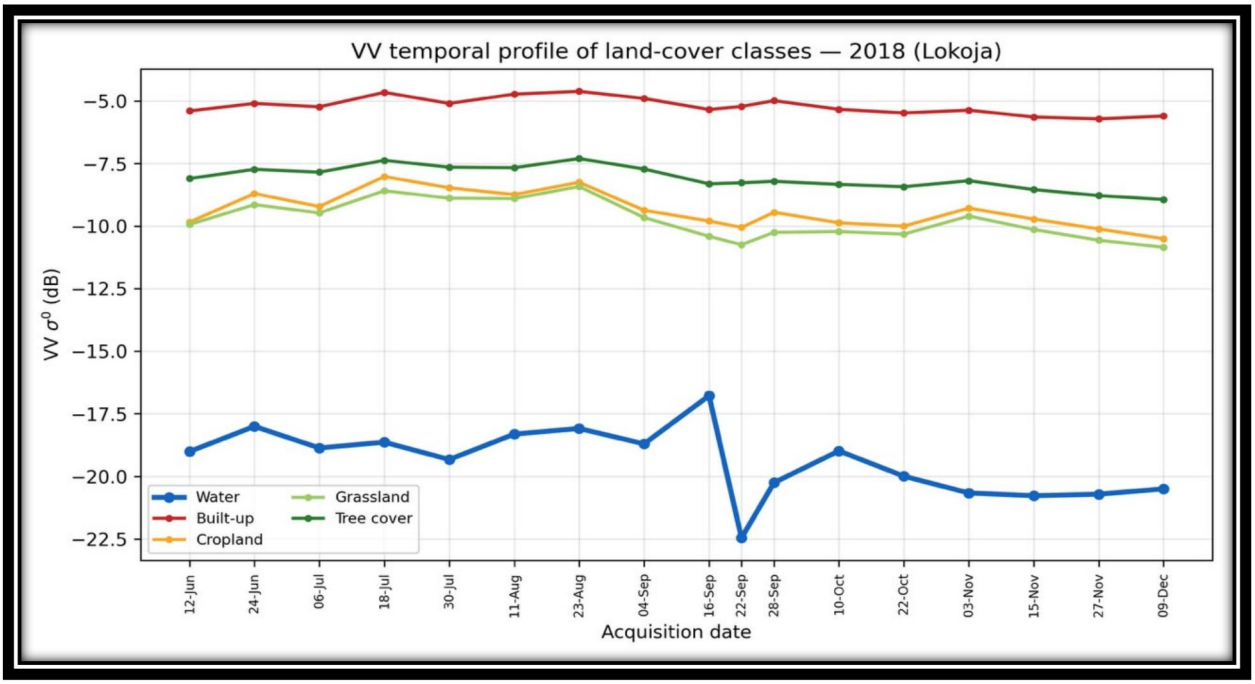


Figure 7a : VV Backscatter time-series and temporal profile of land-cover classes – 2018

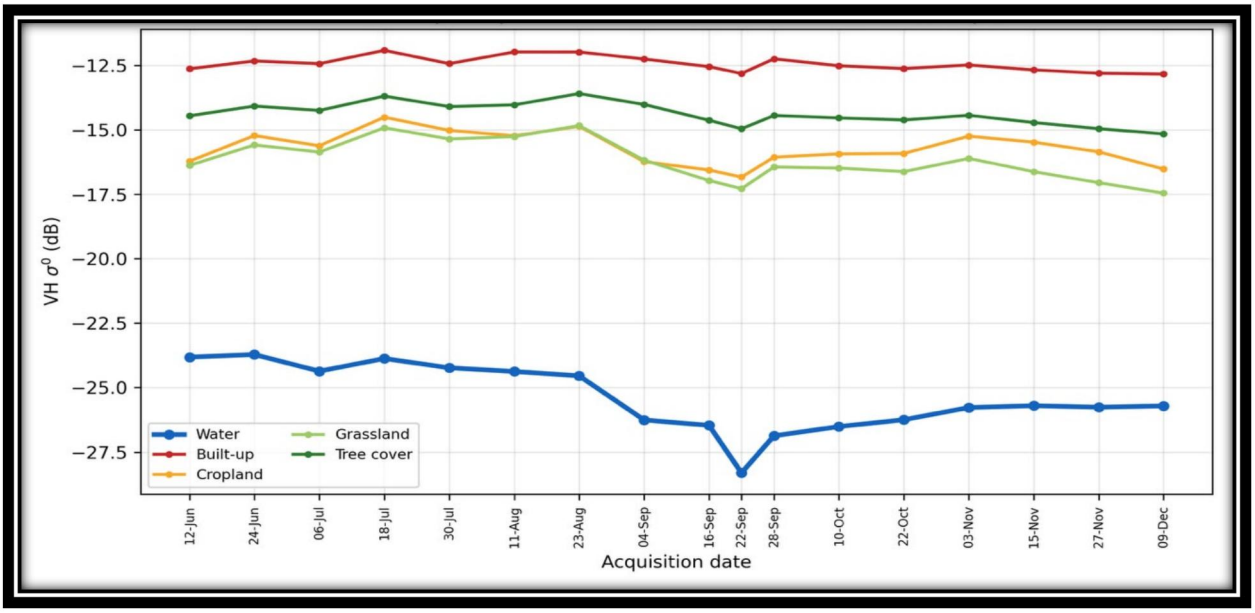


Figure 8a : VH Backscatter time-series and temporal profile of land-cover classes – 2022

4.3 Land-cover Impact

Cropland accounted for 68.5% (135.94 km²) of the 2018 flooded area and 70.2% (193.98 km²) of the 2022 flooded area (Tables 2 and 3). These percentages describe the composition of the inundated zone, not the fraction of all cropland that was flooded. Grassland and herbaceous wetland were the next most affected classes. Built-up areas occupied only 1.5–2.0% of the flooded extent but represent concentrated socio-economic exposure.

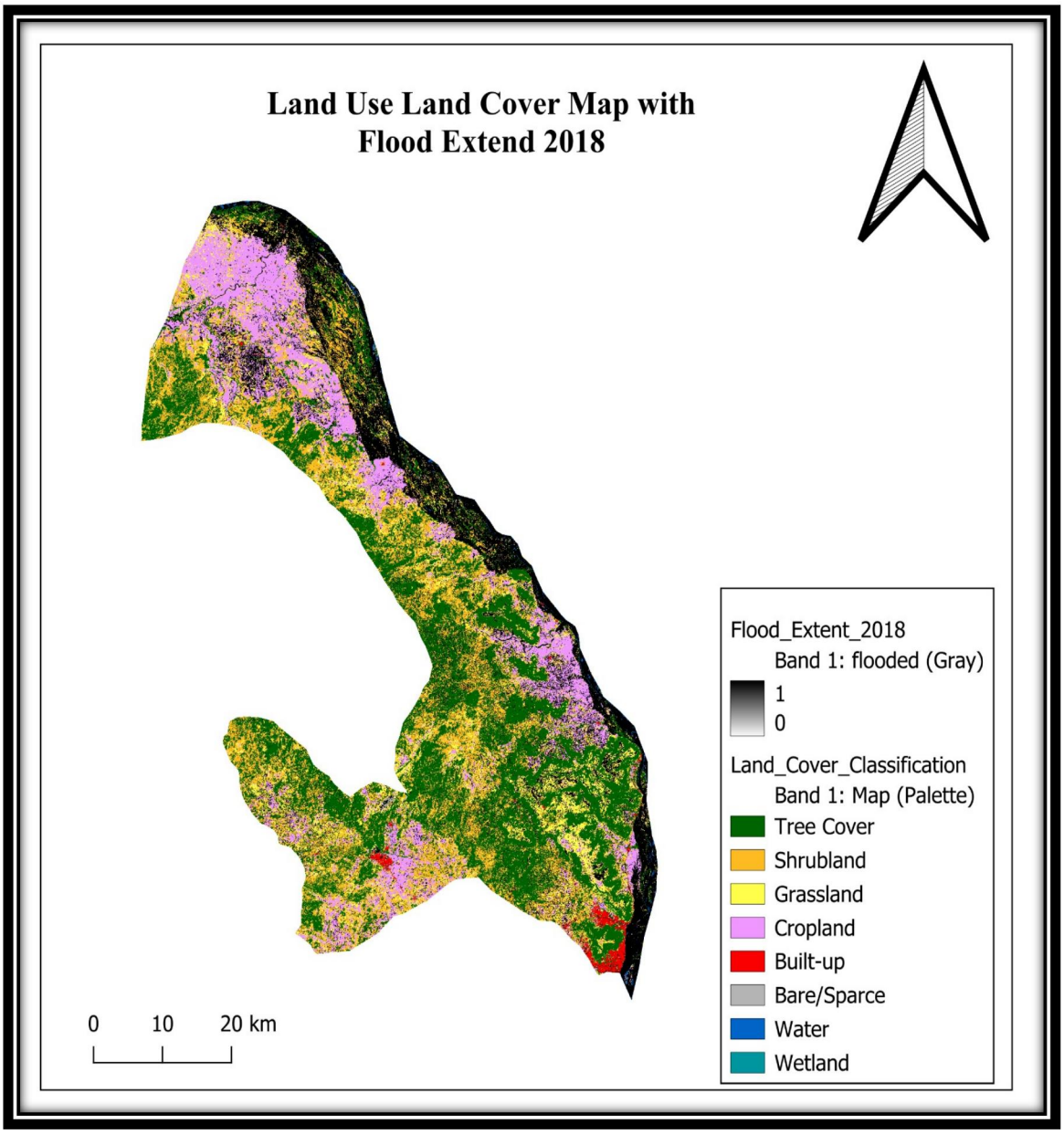
Table 2: Flood impact by land-cover class (2018)

Land Cover Class	Flooded Area (km²)	Percentage of flooded area (%)
Cropland	135.94	68.5
Grassland	31.75	16.0
Herbaceous wetland	17.86	9.0
Tree cover	8.93	4.5
Built-up	2.98	1.5
Shrubland	0.99	0.5
Total	198.45	100.0

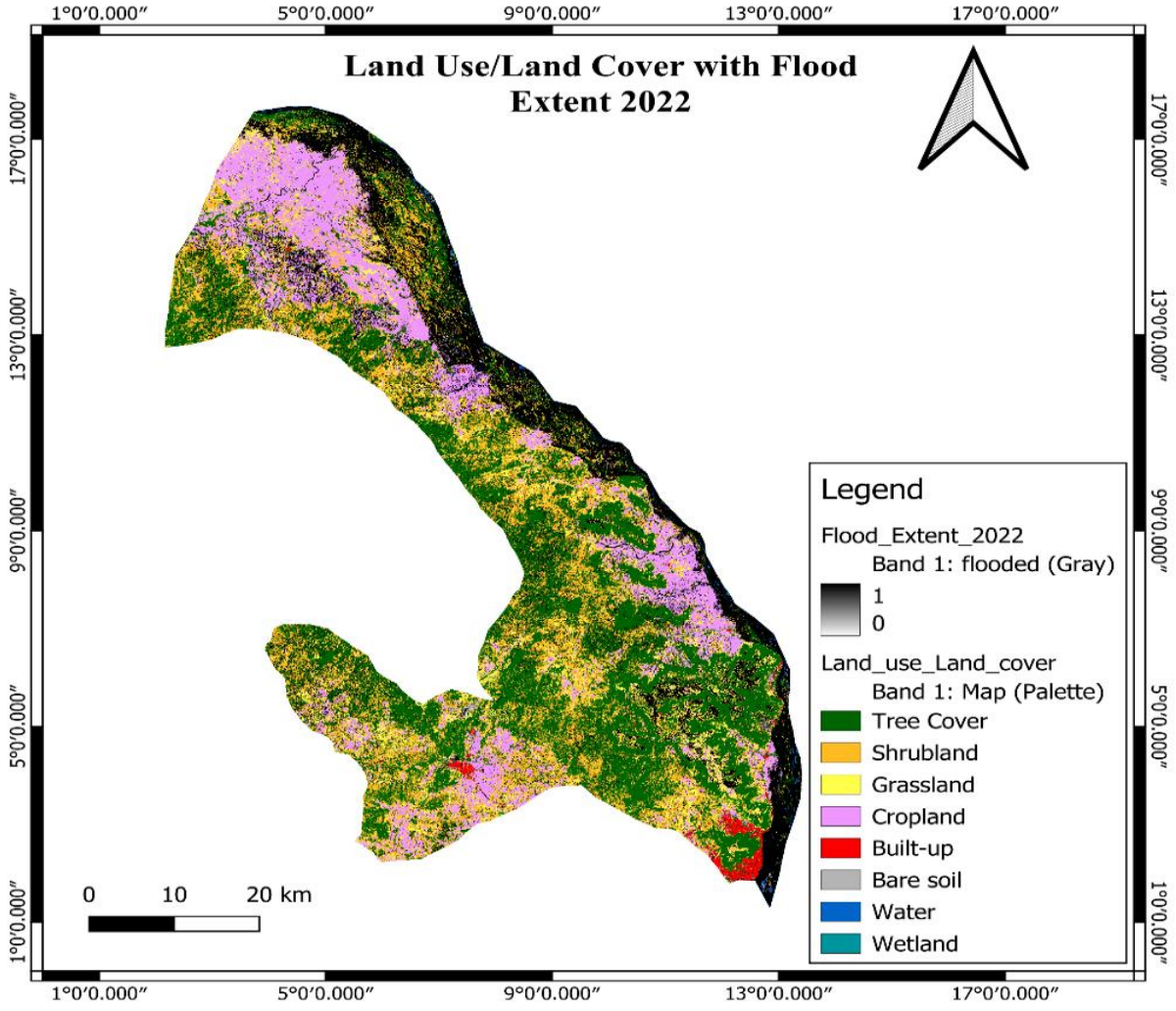
Table 3: Flood impact by land-cover class (2022)

Land Cover Class	Flooded Area (km²)	Percentage of flooded area (%)
Cropland	193.98	70.2

Grassland	42.28	15.3
Herbaceous wetland	22.11	8.0
Tree cover	11.05	4.0
Built-up	5.53	2.0
Shrubland	0.83	0.3
Bare/sparse vegetation	0.55	0.2
Total	276.32	100.0



Figures 8: LULC impact map for 2018



Figures 9: LULC impact map for 2022

4.4 Flood Susceptibility

Approximately 24% of the study area (Very High 12.0% + High 11.5% = 747 km² of 3,181 km²) was classified as high or very high susceptibility (Table 4). These zones concentrate along the low-lying floodplains of the Niger–Benue confluence. The susceptibility map is a separate product from the event-specific flood extent maps.

Table 4: Flood susceptibility zone distribution

Susceptibility Zone	Area (km²)	Percentage (%)
Very High	382.0	12.0
High	365.0	11.5

Moderate	721.0	22.7
Low	1,013.0	31.8
Very Low	700.0	22.0
Total	3,181.0	100.0

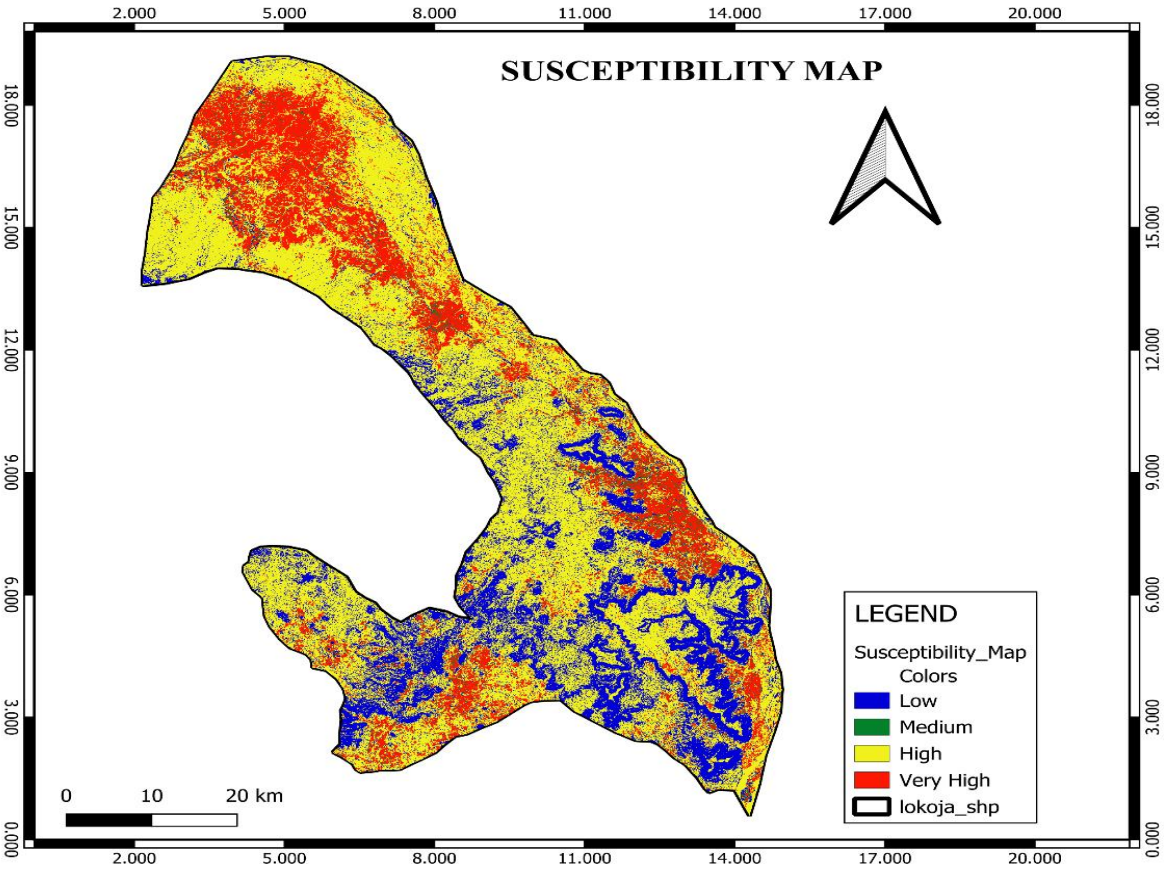


Figure 10: Flood susceptibility map

4.5 Accuracy Assessment

The confusion matrix for the 2022 flood extent map is shown in Table 5. From these values the calculated metrics are:

Table 5: Confusion matrix for 2022 flood extent map

	Reference Flooded	Reference Non-Flooded	Row Total
Classified Flooded	126 (TP)	24 (FP)	150
Classified Non-Flooded	24 (FN)	126 (TN)	150
Column Total	150	150	300

Overall Accuracy = (126 + 126) / 300 = 84.0%.

Producer's Accuracy (Flooded) = 126 / (126 + 24) = 84.0%.

User's Accuracy (Flooded) = 126 / (126 + 24) = 84.0%.

Producer's Accuracy (Non-Flooded) = 126 / (126 + 24) = 84.0%.

User's Accuracy (Non-Flooded) = 126 / (126 + 24) = 84.0%.

Because the matrix is perfectly balanced, all class-specific accuracies equal the overall accuracy. Cohen's Kappa is calculated as:

$P_o = 0.84$; $P_e = 2 \times (0.5 \times 0.5) = 0.50$; $\kappa = (0.84 - 0.50) / (1 - 0.50) = 0.68$.

The Kappa is therefore 0.68. The value indicates substantial agreement beyond chance (Landis & Koch, 1977).

5.0 Discussion

The 39.2% increase in integrated flood extent between 2018 and 2022 is consistent with reports of higher river discharges and prolonged elevated water levels in 2022 (NEMA, 2022). Upstream releases from Lagdo Dam and above-average rainfall in the Benue catchment are documented contributing factors (NEMA, 2022, 2023). Continued cultivation and settlement within the active floodplain further reduce natural storage capacity (Adelekan, 2020). While the present analysis does not include independent discharge hydrographs, the spatial expansion toward Koton-Karfe and Ibaji aligns with the observed increase in inundated area.

The superior performance of VH for open-water detection and the complementary role of VV in vegetated and built-up margins confirm the value of dual-polarisation analysis (Li et al., 2020; Cao et al., 2024). The persistent dominance of cropland within the inundated zone (=70%) underscores the high agricultural vulnerability of the Niger–Benue confluence (Isiaka et al., 2023; Agada et al., 2019). The susceptibility map, covering the full 3,181 km² study area, provides an independent spatial basis for zoning and prioritisation of interventions and should not be confused with the event-specific flood extent products.

The Kappa of 0.68, together with 84% overall accuracy, indicates that the SAR-derived flood extent maps are sufficiently reliable for operational use under cloudy conditions, while also highlighting residual uncertainty arising from flooded vegetation, wind-roughened water and limited ground access during peak flood.

6. Conclusion and Recommendations

This study has shown that Sentinel-1A SAR, processed with dual-polarisation Otsu thresholding, change detection and post-processing, can produce reliable flood extent maps for Lokoja under cloudy conditions. Flood extent increased from 198.45 km² (2018) to 276.32 km² (2022). Cropland consistently dominated the inundated area. Approximately 24% of Lokoja LGA falls within high or very high susceptibility zones. Accuracy assessment of the 2022 extent map yielded 84% overall accuracy and a Kappa of 0.68.

On the basis of the verified findings, the following practical recommendations are offered:

1. Flood monitoring and early warning – Kogi State Emergency Management Agency (SEMA) and the National Emergency Management Agency (NEMA) should integrate routine Sentinel-1 processing (via Google Earth Engine or equivalent) into operational early-warning systems for the Niger–Benue confluence.

2. Floodplain zoning – The high and very high susceptibility zones identified in this study should be adopted by the Kogi State Ministry of Lands, Housing and Urban Development as the spatial basis for restricted development and enforcement of floodplain regulations.

3. Agricultural preparedness – Agricultural extension services should promote flood-tolerant crop varieties, adjusted planting calendars and, where feasible, relocation of the most vulnerable farms out of the recurring inundation zones.

4. Infrastructure and structural measures – Priority investment in embankments, improved drainage and elevated access routes should focus on the recurring flood zones near the confluence and the southern expansion corridor toward Koton-Karfe and Ibaji.

5. Future research – Subsequent studies should incorporate contemporaneous optical imagery (when available), hydrological discharge records, and multi-date land-cover data to further refine both extent mapping and susceptibility modelling.

References

Adelekan, I. O. (2020). Flood risk management in African cities. Natural Hazards Review, 21(4), Article 04020032. https://doi.org/10.1061/(ASCE)NH.1527-6996.0000402

Agada, S., Nirupama, N., & Khalafzai, A. K. (2019). Satellite-based flood mapping for impact assessments: A case study in Lokoja, Kogi State, Nigeria. International Journal of Disaster Risk Reduction, 40, Article 101250. https://doi.org/10.1016/j.ijdrr.2019.101250

Bonafilia, D., Yang, J., Sun, M., & Tellman, B. (2024). A global flood extent map from 10 years of Sentinel-1 SAR data. Nature Communications, 15, Article 10973. https://doi.org/10.1038/s41467-024-54985-6

Cao, H., Zhang, H., Wang, C., & Zhang, B. (2024). Flood inundation mapping in SAR images based on nonlocal polarization combination feature. Journal of Hydrology, 638, Article 131522. https://doi.org/10.1016/j.jhydrol.2024.131522

Ebinne, E. S., Ojima, I. A., & Edebo, J. A. (2019). Satellite-based flood mapping for impact assessments: A case study in Lokoja, Kogi State, Nigeria. International Journal of Advances in Science Engineering and Technology, 7(2), 6–9.

European Space Agency. (2023). Sentinel-1 user handbook. ESA Publications.

Isiaka, I. O., Ajadi, S. A., Arowolo, S. A., Mustapha, S. O., Ndukwe, K. O., & Oluoma, C. C. (2023). Flood impact assessment in Koton Karfe using Sentinel-1 synthetic aperture radar (SAR) data. International Journal of Environment and Geoinformatics, 10(4), 64–76. https://doi.org/10.30897/ijegeo.1348753

Landis, J. R., & Koch, G. G. (1977). The measurement of observer agreement for categorical data. Biometrics, 33(1), 159–174.

Lang, F., Zhu, Y., Zhao, J., Hu, X., Shi, H., Zheng, N., & Zha, J. (2024). Flood mapping of synthetic aperture radar (SAR) imagery based on semi-automatic thresholding and change detection. Remote Sensing, 16(15), Article 2763. https://doi.org/10.3390/rs16152763

Li, Y., Martinis, S., Plank, S., & Ludwig, R. (2020). Optimizing flood mapping using multi-synthetic aperture radar constellations: An operational service chain. European Journal of Remote Sensing, 53(1), 158–171. https://doi.org/10.1080/22797254.2020.1859340

Martinis, S., & Rieke, C. (2015). Backscatter analysis using multi-temporal and multi-frequency SAR data in the context of flood mapping at River Saale, Germany. Remote Sensing, 7(11), 14248–14272. https://doi.org/10.3390/rs71114248

National Emergency Management Agency. (2022). 2022 flood situation report in Kogi State. NEMA.

National Emergency Management Agency. (2023). National flood disaster statistical bulletin. NEMA.

Pulvirenti, L., Chini, M., Pierdicca, N., & Boni, G. (2024). Flood detection with SAR: A review of techniques and datasets. Remote Sensing, 16(4), Article 656. https://doi.org/10.3390/rs16040656

Shen, X., Anagnostou, E. N., Allen, G. H., Brakenridge, G. R., & Kettner, A. J. (2019). Near-real-time non-obstructed flood inundation mapping using synthetic aperture radar. Remote Sensing of Environment, 221, 302–315. https://doi.org/10.1016/j.rse.2018.11.008

Tsyganskaya, V., Martinis, S., Marzahn, P., & Ludwig, R. (2018). Detection of temporary flooded vegetation using Sentinel-1 time series data. Remote Sensing, 10(8), Article 1286. https://doi.org/10.3390/rs10081286